

BRANDEIS UNIVERSITY

DEPARTMENT OF PHYSICS

SENIOR THESIS

Multiflows and Entanglement Entropies in AdS/CFT

Author:
Jesse HELD

Advisor:
Dr. Matthew HEADRICK

May 10, 2019



Abstract

A recent development in the study the AdS/CFT correspondence is that of 'bit threads,' which describe the physical distribution of entanglement in CFTs while simultaneously computing entanglement entropies. Equivalently, we may work with a set of divergenceless vector fields with a collective norm bound called a 'Multi flow.' Via analytic ansatz and numerical computation, we demonstrate that the multi flow formalism fails to compute entanglement entropies for crossing boundary regions. We also present two proofs for the assertion that in the absence of crossing boundary regions there exists a multi flow which computes the entropy of entanglement for an arbitrary number and arrangement of boundary regions.

Contents

1	Introduction	1
2	Background	3
2.1	AdS/CFT and Holographic Entanglement Entropy	3
2.1.1	AdS/CFT	3
2.1.2	Entanglement and Entropy	4
2.1.3	Entropy Inequalities and the Holographic Entropy Cone	6
2.2	The Max-Flow Min-Cut Theorems	6
2.3	Further Connections to Graphs	9
3	Multi flows for Non-Crossing Regions: The Weak Continuum Locking Theorem	10
3.1	Proof by Dualization	11
3.2	Proof by Decomposition	14
4	Multi flows for Crossing Regions	16
4.1	Analytic Attempt: Primal	17
4.2	Analytic Attempt: Dual	19
4.3	Numerical Check: Dual	21
4.3.1	Implementation	21
4.3.2	Results	22
4.4	Numerical Check: Primal	23
4.4.1	Implementation	23
4.4.2	Results	26
5	Discussion and Future Work	26
6	Acknowledgements	29
7	References	29

1 Introduction

The apparent emergence of duality between Conformal Field Theories (CFTs) and Anti-de Sitter (AdS) Space of one higher dimension is a topic of great interest in high energy physics. A CFT

is a quantum field theory which exhibits conformal symmetry and AdS is a maximally symmetric space-time with a constant negative curvature. The equivalence between these systems is referred to as '*holographic*' since the AdS is of one higher dimension than the CFT. This allows us to think of the CFT as existing on the boundary of the holographic AdS, which we refer to as *the bulk*. This duality, referred to as the AdS/CFT Correspondence, gives theorists a unique framework in which to explore a number of open questions in a variety of fields, from condensed matter to quantum gravity.

The work presented here concerns itself primarily with the study of information and entanglement on states of Conformal Field Theories. Our main interest is in developing methods of calculating the entropy of entanglement between different spacial regions of CFTs, giving us a means of probing the information structure of holographic states and determining some shared properties of all holographic states. As the study of the AdS/CFT Correspondence has progressed, the Ryu-Takayanagi (RT) formula has become widely accepted as a means of calculating the entanglement entropy. The RT formula relates the entropy of a region of the boundary CFT to the area of the minimal surface homologous to this region in the bulk AdS space. The RT formula, while useful, gives us a very limited intuitive sense of the physical structure of the underlying state.

In order to increase our understanding of the information structure of holographic states, consider the following picture:

Threads with a certain cross-sectional area are placed onto the some region A of the boundary CFT and are allowed to run through the bulk and onto some point of the boundary within the complement of A . In this picture, the minimal surface referenced by the RT formula above acts as a bottle-neck for such threads and thus the maximum number of such threads which can connect A to its complement also gives us the entropy by revealing the area the minimal bulk surface homologous to A in an indirect fashion. Each individual thread can be thought of as entangling two separate points on the CFT and each carries an entropy equivalent to that of a maximally entangled Bell Pair, and thus we refer to these threads as *bit threads*.

The equivalence between the RT formula and this bit thread picture is realized as a continuum version of the *max-flow min-cut theorem* from graph theory by using techniques from the theory of convex optimization. In particular, the strong duality of convex optimization problems allows us to equate the RT formula to a new problem in which we try to maximize the number of bit threads connecting a region to the rest of the boundary CFT.

While the bit threads serve as an excellent tool to inform our intuition, they are not particularly useful for doing calculations. In order to find some middle ground between the physically informative and the computationally useful, we can think of bit threads as microscopic (and in fact Planck-scale) objects and work in a course grained picture where we work with a vector field with certain properties referred to as *flow*. In order to maintain the physical properties of the microscopic bit threads, these fields must be divergenceless and have a bounded norm. The condition that the field is divergenceless says that every thread must begin and end on the boundary CFT and no thread can spontaneously appear or disappear in the bulk. The bound on the magnitude of the field is effectively a statement that the threads have spacial extent and thus cannot occupy more volume than is available to them. This flow can be interpreted as an information flux density, the field lines of which are followed by the bit threads. This lets us go back and forth freely between the thread and flow based picture.

The flow field is easier to work with than the threads for the means of computation, and since a given field configuration is easily converted into a thread configuration flows can also serve as a visual aid for understanding the spacial distribution of entanglement. A flow field, however,

can only compute the entropy of a single region or at most, regions nested inside of one another. In order to find the entropies of more complicated arrangements of boundary regions we need something else. Once again, graph theory provides the inspiration we need.

On graphs, there is a class of problems which are referred to as 'multi-commodity flow problems' or 'multi flow problems' for short. These problems are a fairly straight-forward extension of single commodity flow problems (which were the inspiration for flows in the continuous system). Essentially, a multi-commodity flow is just a number of single commodity flows on the same graph at the same time. Thus we can define a continuum multi flow as a set of vector fields which are divergenceless and obey a bound on the sum of their magnitudes. Each field in a multi flow translates to a configuration of threads connecting a pair of regions, and together, the multi flow as a whole represents threads connecting any number of regions to one another.

The multi flow formalism has proven useful as a computational tool, and we would like to see just how useful it could be. Its derivation from its counterpart on graphs leads us to believe that many results for the graph based multi flows should be true in the continuum. In particular, results which tell us the computational limits of multi flows on graphs may apply in the continuum. If these same limits apply for the continuum multi flows, we can use graph based problems to model those in the continuum AdS/CFT. This would allow us to apply techniques and algorithms already formulated for the RT prescription to multi flows, giving us the ability to generate and prove a list of inequalities obeyed by the entropies of holographic states for any number of regions of the CFT [1]. We could then use the multi flow picture to analyze the physical meaning of these inequalities and probe the information structure of holographic states. This goal is a ways away, and first we must check to see if this is possible by finding the computational limits on multi flows. This is the goal of the work presented here.

To begin, we provide a more technical introduction to the concepts introduced here in the next section and elaborate on some of the connections between entanglement entropies and graph theory. In section 3 we go onto generalize previous results pertaining to multi flows before analytically and numerically approaching a toy problem in section 4 which will illustrate that multi flows cannot be used to calculate the entropy of crossing regions. This will represent the point at which the analogy between our constructs in AdS/CFT will diverge from their analogs on graphs.

2 Background

2.1 AdS/CFT and Holographic Entanglement Entropy

2.1.1 AdS/CFT

The AdS/CFT Correspondence is as powerful as it is because it tells us that two systems, which on the surface appear to be very different, are equivalent. This fact allows us to take many difficult calculations from one system and perform them much more easily in its dual description. We will be performing a very complicated CFT calculation with relative ease in the dual AdS.

Recall that AdS or Anti-de Sitter space-times are maximally symmetric space-times with a constant negative curvature. This means that the length element approaches zero at infinity, which will cause problems. In order to get around this, we impose a cutoff to the AdS which is associated with the length-scale down to which we trust the physics in our CFT. Doing this gives us a bounded manifold, which we denote \mathcal{M} . Another important note about the AdS in 'AdS/CFT' is that it need not be simple, empty Anti de-Sitter space. Different states of the boundary CFT

have different holographic duals which are *asymptotically AdS*. A holographic state may have an asymptotically AdS dual that contains matter, energy, black holes, etc.

On the other side of the equation, we have states of quantum field theories with conformal symmetries. These aforementioned 'holographic states' are not just any random state of the field theory. Rather, we restrict ourselves to working with these special states that have well defined asymptotically AdS dual space-times associated with them.

Our goal will be to study the structure of these *holographic states* in order to learn what features of these states are important for holography. Examining entanglement in these states is one way we can do this. This is because holographic states all obey certain inequalities which can give us insight into their structure and hint towards how asymptotically Anti-de Sitter Spaces emerge from them. We will discuss these inequalities later in this section.

2.1.2 Entanglement and Entropy

Entanglement is a fundamental feature of quantum mechanics. This phenomenon is one of the few ways in which physicists may encode information in quantum systems without that information becoming lost to the uncertainty built into quantum mechanics.

The AdS/CFT Correspondence gives us the ability to study the structure of entanglement within quantum systems with infinite degrees of freedom. Studying entanglement will lead to a better understanding of how to manipulate information in quantum systems, as well as how entanglement may be connected to the emergence of gravitational systems.

Holographic states, like all quantum states with many degrees of freedom, can be described entirely by the operator which is often known as the density matrix operator. In order to examine the entanglement which is internal to this state, we must first divide it into parts. The simplest way of doing this is to consider a region A of the conformal field theory and ask how the state on only that region is entangled with the rest of the field theory A^c . The state on A is described by the reduced density matrix, given by:

$$\rho_A = Tr_{A^c}[\rho] \quad (1)$$

where Tr_{A^c} represents the partial trace over the degrees of freedom in A^c .

The entanglement across a partition of the state can be quantified by an entropy, which can be used to tell us (practically speaking) how much information is stored in the entanglement between the bipartite regions. This *entanglement entropy* is given by the von Neumann entropy, which for a region A is

$$S(A) := -Tr[\rho_A \ln(\rho_A)] \quad (2)$$

From the definition above, one can define a number of useful quantities by taking the sums and differences of entropies of different regions in a multipartite system. These more directly reflect the amount of information which is, or is not shared between regions of the boundary CFT.

As of yet, there has been no mention of the space-time of one higher dimension beyond the conformal field theory. The most relevant connection between from a CFT to its holographic dual is given by the RT formula, which gives a method for finding the von Neumann entropy via geometric calculation in an asymptotically Anti-de Sitter space. The RT formula equates the von Neumann entropy of a region A with the area of the minimal surface in the bulk that is homologous to A . In mathematics, this stated as:

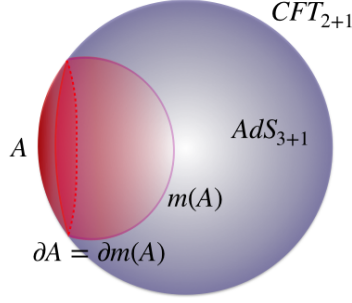


Figure 1: A visual illustration of the RT formula for $CFT_{2+1}=AdS_{3+1}$. The entropy of a region A of the CFT is equivalent to the area of the minimal surface $m(A)$ in the bulk AdS such that the boundary of the surface is the same as that of the region A

$$S(A) = \frac{1}{4G_N} \text{Area}(m(A)) \quad (3)$$

where $m(A)$ denotes this minimal surface.

There is an alternative version of the RT formula which is described in terms of a vector field in the bulk. Such a vector field v is referred to as a *maximal flow* and obeys the following constraints:

$$\begin{aligned} r \cdot v &= 0 \\ |v| &= 1 \end{aligned} \quad (4)$$

for the reasons outlined in the introduction. We refer to a flow as maximal (for a region A) when:

$$\int_A \rho_{-} \frac{1}{h} v \cdot n = S(A) \quad (5)$$

where h is the determinant of the induced metric on the boundary A and n is the unit vector normal to A . The reason that these are called maximal flows will be described later in this section.

One subtlety of this formalism is that the bit threads are undirected while the flow field is. By convention we will always have a flow going out of the region it is associated with and into its complement.

Single flows present an interesting conceptual alternative to the RT formula although they do not tell us anything more than the RT formula when it comes to the entanglement structure of holographic states. In order to learn more about this particular topic, we need to know how threads must be distributed across multiple regions. The flow formalism is insufficient to do this calculation, so we can give it an upgrade and define what we call a *multi flow* $\vec{v}_{ij}g$, which is simply a collection of individual flow fields v_i which together obey a collective norm bound

$$\sum_i |v_i| = 1 \quad (6)$$

If a multi flow is maximal for some set of boundary regions A_i , then we define the flow going from A_i to A_j as v_{ij} , then the multi flow is given by $\vec{v}_{ij}g$. Notice that some additional constraints follow immediately from this setup:

$$v_{ij} = -v_{ji} \quad (7)$$

$$\forall_{ij} \quad \hat{n}_k = 0 \quad \partial k \notin i;j$$

where \hat{n}_k is the normal vector to the region A_k . Multi flows have the potential to let us map out the entanglement structure of holographic states, which was not previously possible with the RT formula or the single flow formalism. For this reason, the multi flow structure is of great interest and so it is the subject of the work performed herein.

2.1.3 Entropy Inequalities and the Holographic Entropy Cone

The RT formula in its various forms allows us to probe the entanglement structure of holographic states (since it is necessarily holographic calculation). By examining the entropy of multiple regions of a CFT in a general holographic state, we can determine some features of the entanglement structure that make it holographic. While a few facts are immediately obvious from the definition of the entanglement entropy in terms of CFT calculations, many more conditions on holographic states emerge once the RT formula comes into play. Two prominent entropy inequalities are

$$\begin{aligned} S(AB) + S(BC) &\geq S(B) + S(ABC) \\ S(AB) + S(BC) + S(AC) &\geq S(A) + S(B) + S(C) + S(ABC) \end{aligned} \quad (8)$$

Where $AB; BC; ABC$, etc. are the unions of the respective regions $A; B; C$, etc. These inequalities are known as *strong subadditivity* (SSA) and *the monogamy of mutual information* (MMI) respectively.

If we consider n regions of the CFT, we can construct a vector in $\mathbb{R}^{2^n - 1}$, the elements of which are the entropies for each region and all possible combinations of them. As discussed in [1] in this space, referred to as the *holographic entropy cone for n regions*. The extremal rays defining the edges of the holographic entropy cone are those entropy vectors for which some entropy inequality is saturated. It turns out that for $n \leq 4$ SSA, MMI, and other inequalities which can be derived from the two taken together, completely define the holographic entropy cone. However, for $n = 5$ there are more inequalities which constrain holographic states. Using the minimal surface prescription, a method has been constructed for finding and proving such higher-party entropy inequalities [1]. For this to be accomplished, it is necessary to construct a *graph model of holographic entanglement entropies*. An example of a more complicated entropy inequality is

$$\begin{aligned} S(ABC) + S(ABD) + S(ABE) + S(ACD) + S(ACE) + S(BC) + S(DE) \\ S(AB) + S(ABCD) + S(ABCE) + S(AC) + S(ADE) + S(B) + S(C) + S(D) + S(E) \end{aligned} \quad (9)$$

which is one of the entropy inequalities for five regions which is independent of SSA and MMI.

The typical procedure for proving entropy inequalities using bit threads, is to find a maximal flow or multi flow for all regions that appear on the right hand side, and then show that the inequality follows as a consequence of the thread configuration. We will see that this is not a trivial task for inequalities of this form because the right hand side contains *crossing regions* (for example AC and ADE). If we want to use the multi flow formalism to prove and analyze these inequalities, this must be addressed.

2.2 The Max-Flow Min-Cut Theorems

The flow and multi flow formalism is constructed formally by moving a theorem for graph based multi flows into the continuum. This theorem is the well known *Max-Flow Min-Cut Theorem*

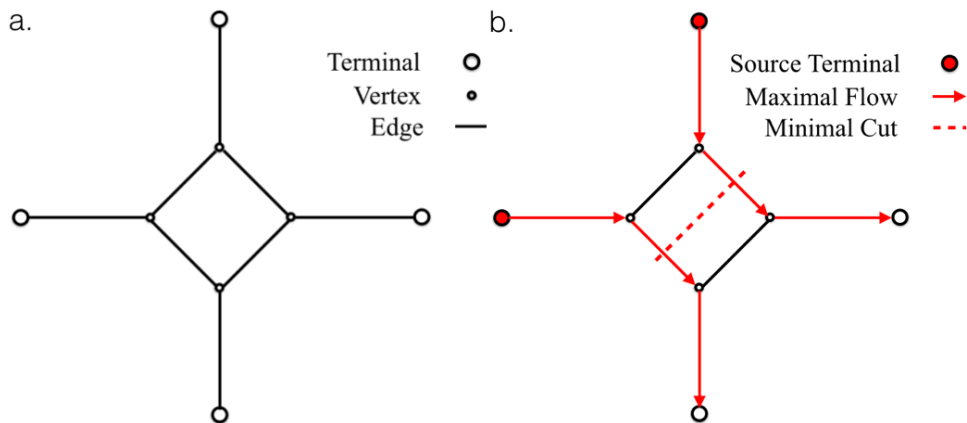


Figure 2: a.) An example graph on which we may define a commodity flow problem. This graph is made up of vertices connected by edges, some subset of which are declared to be the 'terminals' of the graph which will act as sources or sinks for the commodity flow. b.) Example of a commodity flow program where the commodity is sent from source terminals through the graph to the remaining terminals. The Max-Flow Min-Cut Theorem states that the maximum flow that can be sent from some source terminals is equal to the minimum number of edges which are cut by a partitioning of the vertices such that the source terminals are separated from the rest in the partition.

(MFMC). A brief visual explanation of the graph based MFMC Theorem is presented in Figure 2. The graph presented in the figure has all edges with a capacity of 1, however in general one can weight edges differently such that more or less flow can pass through one edge than others. We call these weights the *capacity* of an edge. The only thing this changes on the cut side is that the minimal cut is now computed by the sum of the capacities of the edges cut by the partition. It should be noted that any commodity flow must be conserved at every vertex and no commodity flow can exceed the capacity of the edge it passes through.

Flows are a continuum analog of the single commodity flow on graphs, and likewise multi flows are a continuum analog of multi-commodity flows on graphs. Instead of conserving flow at vertices, we now demand that all flow fields are divergenceless in the bulk. Similarly, instead of forcing commodity flows to respect the capacity of the edges they traverse, we now demand that the magnitude of flow fields do not exceed some bound.

The equivalence between maximizing the flux of a vector field across a source region of a continuous boundary and minimizing the area of a surface homologous to the source region is referred to as the continuum MFMC Theorem and is proven using the strong duality between convex programs. A convex program is the statement of an optimization problem of a certain form. The components of a convex program are:

1. $f(x)$: Some variables defining a convex set over which the optimization will occur
2. $f_0(f(x))$: A convex or concave function which is referred to as the objective of the program. This function will be minimized (or maximized in the case of a concave function) subject to some constraints.

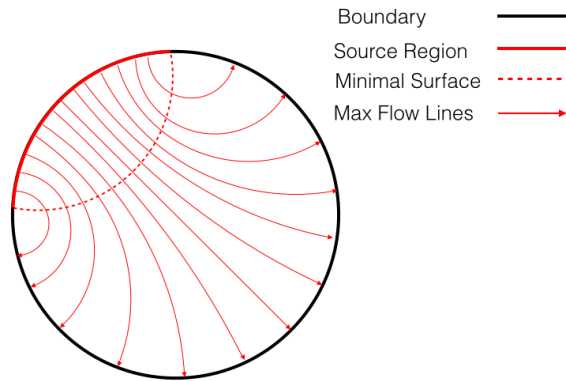


Figure 3: An illustration of the continuum Max-Flow Min-Cut Theorem. In place of source terminals we now have a source region (or set of source regions). The commodity flow is replaced by a norm-bounded, divergenceless vector field and the minimal cut is replaced by the minimal surface homologous to the source region

3. $f_i(\mathcal{F}Xg)$: A set of convex inequality constraints of the form $f_i(\mathcal{F}Xg) \leq 0$.
4. $h_i(\mathcal{F}Xg)$: A set of affine equality constraints of the form $h_i(\mathcal{F}Xg) = 0$.
Taken with the inequality constraints, these define a set of feasible points within the larger space spanned by the variables of the program. The solution to the convex program will be at some point within the set of feasible points.

One important feature of convex programs is that if the set of feasible points is non-empty, the program can be *dualized* by removing the constraints on the program and adding back those constraints, multiplied by Lagrange multipliers, to the program's objective. Once the unconstrained optimization is performed over the original variables, we are left with the objective of a new *dual* program. This is to be optimized with respect to the Lagrange multipliers associated with the original constraints. This new dual program will be a minimization problem if the original, or *primal*, program was a maximization problem. The crucial fact used in proving the equivalence of the flow prescription to the RT formula is that the optimal objective value of these two problems will be the same.

Based on purely geometric arguments, it becomes clear that with flows such that $\int v_j = 1$,

$$\int_A v \cdot S(A) \tag{10}$$

where $\int_A v \cdot S(A)$ is used as a short-hand for $\int_A v \cdot \rho_{-} n$. Now we can write our flow problem as a concave program:

$$\text{Primal: Maximize } \int_A v \text{ with respect to } v, \text{ subject to } \int v = 0 \text{ and } \int v_j = 1: \tag{11}$$

By dualizing this program, we obtain a minimization problem which has a solution bounded below by the entropy of A . Thus the entropy will be the extremal value of both the primal objective and the dual objective:

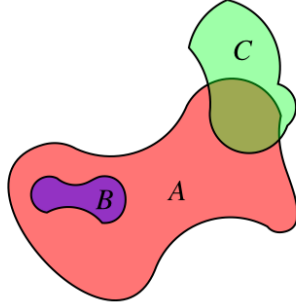


Figure 4: For the three sets $A; B; C$ depicted. A and B do not cross because B is entirely nested within A . B and C do not cross since their intersection is empty. A and C do cross since their intersection is non-empty and neither is a subset of the other.

$$\text{Max}_A \int_A v = S(A) \quad (12)$$

Furthermore, it will turn out that the configuration of variables which extremizes the dual program will return a delta function along the minimal surface homologous to the source region [2].

By extension, the continuum MFMC theorem can be applied to multi flows by a similar procedure. Only in this case, we will include the flux of multiple flows through multiple regions in our primal objective.

2.3 Further Connections to Graphs

Graph theory provides the framework for developing the multi flow formalism, but it also contributes in other ways to the study of entanglement entropy in AdS/CFT. One interesting and relevant example of this is the development of a graph model for holographic entanglement entropies which contains all of the relevant information about the minimal surfaces of source regions and their unions. One reason for this development is so it can be used for an algorithm to find and prove entropy inequalities for multipartite systems, beyond SSA and MMI [1]. Due to their strong connection to graph based problem, it is reasonable to ask if flows and multi flows can be modeled in a similar fashion, and if such machinery can be used in an analogous way to study entropy inequalities.

The continuum and discrete MFMC theorems lead us to believe that the graphs which model cuts and flows should be identical. Now we can turn to known results from graph theory to test how well the multi flow formalism holds up compared to its discrete counterpart.

The particular graph theoretic result is known as the *Locking Theorem*. This tells us if a maximal multi-commodity flow exists given a particular choice of subsets of terminals which we want to maximize the flows from. In particular, the Locking Theorem puts a limit on how sets of source terminals may *cross*. The condition for two regions A and B to be crossing is that none of the following sets are empty:

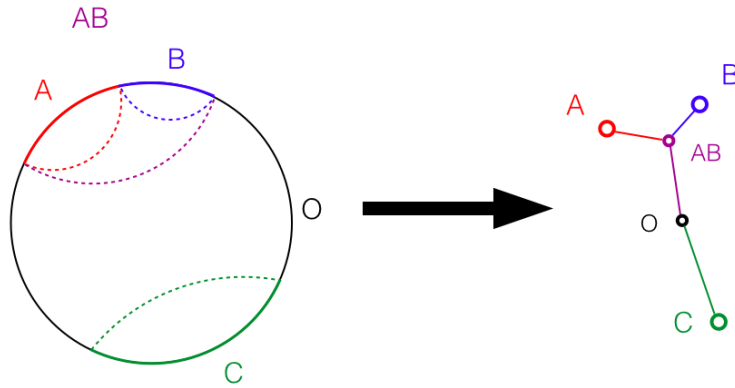


Figure 5: Example of converting a set of source regions with their minimal surfaces into a graph model. The boundary along with the minimal surfaces of source regions divide the bulk into disjoint volumes, each of which is assigned a vertex in the graph model. Each bulk cell is connected to adjacent ones in the graph models via edges which are weighted by the area of their shared boundary (in the example here this is just the area of the minimal surface dividing them).

$$A \setminus B; \quad A=B; \quad B=A; \quad (A \cap B)^c: \quad (13)$$

For simplicity we will usually omit the last condition, as it is meant to exclude cases which do not concern us. The Locking Theorem is stated (in simplified language) as follows;

The Locking Theorem: For any family of 3-cross free subsets of terminals, there exists a multi-commodity flow configuration which simultaneously maximizes the flow from each subset.

For a more in depth treatment of the Locking Theorem, see [3]. In order for the idea of modeling continuum multi flows as discrete multi-commodity flows to work, our continuum construct must also satisfy the Locking Theorem. We will soon see, however, that this is not the case. Before we examine the failure of continuum multi flows to satisfy the Locking Theorem, we should first check that it does not fail in cases which are regarded as trivial by the discrete Locking Theorem, i.e. in the case of non-crossing source regions.

3 Multiflows for Non-Crossing Regions: The Weak Continuum Locking Theorem

As of now, it has been proven that there exists a multi flow which is maximal for:

1. Any number of disjoint source regions
2. Any number of disjoint source regions and one additional *composite* region made up of some union of the other disjoint *elementary* regions [4].

The Locking Theorem states that this should still be true for any arbitrary choice of non-crossing regions or for regions which have crossings but are still 3-cross free. Before we consider whether or not multi flows can reproduce entropies for crossing regions, we must first prove to make sure that this can be done for an arbitrary number of disjoint and nested regions.

In this section, we present two different proofs which show that this is the case. We refer to this result as *the Weak Continuum Locking Theorem* and it can be thought of as a generalization of the Theorems proven in [4] pertaining to multi flows.

3.1 Proof by Dualization

The first proof is accomplished by dualizing the convex program of maximizing a multi flow over arbitrary non-crossing regions. By utilizing equation (10), it is sufficient to show that the objective of the dual program is bounded below by the sum of the entropies of the source regions. We begin by partitioning the boundary into N disjoint regions and labeling these regions A_i . Now define some number of regions $fB \ g$ such that $B = fA_1; A_2; \dots; A_Ng$ subject to the constraint that at least one of the following conditions holds;

$$B \setminus B = ; ; B \ B ; B \ B \ \delta ; \tag{14}$$

which is the statement that these regions are non-crossing. We will refer to these regions as *composite regions*. We now construct a convex program which will maximize the flux of some multi flow over each composite region.

The statement of our program is

$$\text{Primal Program: Maximize } \sum_{A_i \supseteq B} \sum_{A_j \not\supseteq B} \sum_{A_i} v_{ij}; \tag{15}$$

with respect to $f v_{ij} g$, subject to:

$$v_{ij} + v_{ji} = 0; \tag{16}$$

$$\sum_{i < j} v_{ij} = 0; \tag{17}$$

$$\sum_{i < j} j v_{ij} \leq 1; \tag{18}$$

If we define n_{ij} to be the number of sets B which contain A_i and not A_j ($n_{ij} := \#(\{ A_i \supseteq B ; A_j \not\supseteq B \})$) and make use of constraints (5) and (6), we can rewrite the object of the primal program as:

$$\sum_{i < j} \sum_{A_i} n_{ij} v_{ij} - \sum_{A_j} n_{ji} v_{ij}; \tag{19}$$

We can write a Lagrangian for our program by not explicitly enforcing constraints (17) and (18) and instead, add them to our objective multiplied by Lagrange multipliers (γ_{ij} and μ). The Lagrangian is

$$\sum_{i < j} \sum_{A_i} n_{ij} v_{ij} - \sum_{A_j} n_{ji} v_{ij} + \sum_M \mu + \sum_{i < j} \gamma_{ij} \sum_{A_i} v_{ij} - \sum_{i < j} \mu_j \sum_{A_j} v_{ij}; \tag{20}$$

If we perform integration by parts, and then demand that the maximum of the Lagrangian with respect to the multipliers be finite, we obtain our dual program:

$$\text{Dual Program: Minimize } \int_M \dots; \quad (21)$$

with respect to λ_{ij} , subject to:

$$\lambda_{ij} = \lambda_{ji}; \quad (22)$$

$$\lambda_{ij} A_i = \lambda_{ij} A_j = \lambda_{ji} A_i; \quad (23)$$

Notice that (22) and (23) taken together imply that for any path c between A_i and A_j

$$\int_c ds \lambda_{ij} = N_{ij} \quad (24)$$

where $N_{ij} := \lambda_{ij} + \lambda_{ji}$. We then define $N_i := \#\{A_j \supseteq B \mid B \supseteq A_i\}$, which is the number of B which contain A_i and are also contained in B (and note that B is not counted in N_i). In general, we know that

$$N_i + N_j = N_{ij}; \quad (25)$$

By this definition, it follows that

$$\begin{cases} N_i \leq \lambda_{ij} + 1 & A_i \supseteq B \mid A_j \not\supseteq B \\ N_i = 0 & A_i \not\supseteq B \end{cases} \quad (26)$$

where the first inequality relies on the fact that B is not counted in N_i .

We now define functions $\phi_i(x)$:

$$\phi_i(x) := \inf_{c \text{ from } A_i \text{ to } x} \int_c ds; \quad (27)$$

This implies that

$$\phi_i(x) + \phi_j(x) = N_{ij}; \quad (28)$$

Now we define

$$\psi(x) := \min_{A_i \supseteq B} (\phi_i(x) - N_i); \quad (29)$$

and we denote the level sets of these functions as

$$\mathcal{R}(p) := \{x \supseteq M \mid \psi(x) = p\} \quad (30)$$

for some $x \supseteq A_i \supseteq B$, $\phi_i(x) = 0$ and $N_i = 0$. Thus $\psi(x) = 0$ by (29). Now consider a different $x \supseteq A_j \not\supseteq B$, if we let $A_i \supseteq B$ be the minimizer of (29), we know that $\phi_j(x) = 0$ and thus by (28) and (26),

$$\psi(x) = \phi_i(x) - N_i = N_{ij} - N_i = 1 + \lambda_{ji} - 1; \quad (31)$$

Thus, the level sets of ψ between 0 and 1 must be homologous to B . We then define regions

$$R := \{x \in M \mid 0 < \phi(x) < 1\} \quad (32)$$

If all composite regions are non-crossing, then we should expect that

$$R \setminus R = \emptyset \quad (33)$$

if $\phi \in \mathcal{C}^0$. In order to show this, we must consider two cases: one in which $B \setminus B = \emptyset$, and the other where $B \cap B \neq \emptyset$.

1. In the first case, let $B \setminus B = \emptyset$. We will also let $A_i \supseteq B$ such that $\phi(x) = \phi_i(x) - N_i$ and $A_j \supseteq B$ such that $\phi(x) = \phi_j(x) - N_j$ for some x . If we choose x to be some point in R we know that by definition

$$\phi(x) < 1 \quad (34)$$

For this case, we also know that

$$N_i + N_j = N_{ij} + 2 \quad (35)$$

by equation (26). We now note that this, along with (28) and (29), gives

$$\phi(x) + \phi(x) = \phi_i(x) + \phi_j(x) - (N_i + N_j) + 2 \quad (36)$$

and that combining this with (34) implies that

$$\phi(x) > 1 \implies R \setminus R = \emptyset \quad (37)$$

in the case of disjoint composite regions.

2. For the second case, suppose instead that $B \cap B \neq \emptyset$ but still that $x \in R$ and that $A_i \supseteq B$ such that $\phi(x) = \phi_i(x) - N_i$. Then the inequality (34) still holds but instead of (35), we now have

$$N_i = N_i + 1 \quad (38)$$

From the definition of N_i and the premise of the case. This along with (34) implies that

$$N_i + N_j = N_i + N_j = \phi_i(x) - N_i \implies \phi(x) < 0 \implies R \setminus R = \emptyset \quad (39)$$

Thus the claim holds for both cases.

The fact that the R do not intersect allows us to place the following bound on the dual objective:

$$\int_M \phi \times \int_R \phi \leq \int_M \phi \times \int_R \phi \quad (40)$$

Now using Hamilton-Jacobi theory (taking $\int_c ds$ to be the action), we find that $\phi = \int_R \phi(x) j$ thus we can rewrite this as:

$$\int_M \phi \times \int_R \phi = \int_M \int_R \phi(x) j \quad (41)$$

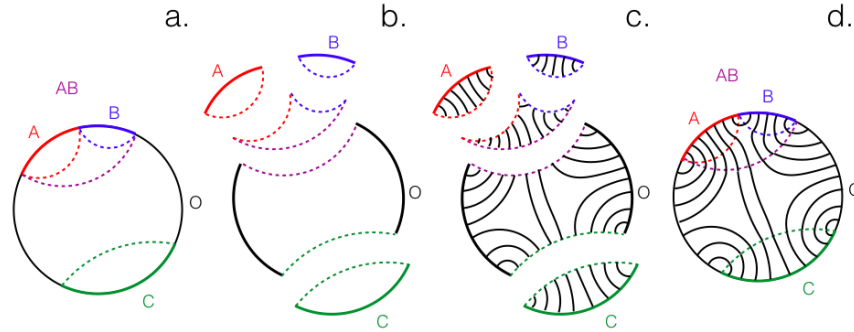


Figure 6: Illustration of the proof by decomposition. a) depicts step 1; the choice of source boundary regions and the identification of their minimal surfaces. b) depicts step 2; the dividing of the bulk into cells. c) depicts step 3; finding a maximal thread configuration for the boundaries of each bulk cell, and lastly d) depicts step 4; in which the bulk cells are recombined to obtain a maximal thread configuration for the original problem identified in step 1.

Since the integrals on the RHS correspond to the average area of the level sets of ϕ homologous to B they must be at least as great as the area of the minimal surface homologous to B . So:

$$\int_M \langle \phi \rangle \times \int_R \langle \phi \rangle \geq S(B) \quad (42)$$

by the RT formula. However by strong duality, the minimum of the LHS, subject to the correct constraints, must be equal to the optimum of the primal program. Thus the flux of the multi flow from all B is both bounded above and below by the sum of their entropies, and thus we can conclude that there exists a multi flow which is maximal for all B so long as there is no crossing between them.

3.2 Proof by Decomposition

In addition to the proof above, which relies on computing the dual program and constraining it's solution, we provide a second proof. Rather than relying on the formal theory of convex programs, this proof will be a proof by construction. We will present a method for constructing a multi flow which saturates on the minimal surfaces of all chosen boundary regions, and thus can be used to simultaneously calculate their entropies. To avoid confusion regarding orientation, we will proceed by talking mainly in the language of bit threads, knowing that once we have finished constructing a thread configuration it can be converted into a proper multi flow.

The procedure for constructing a maximal multi flow for any set of non-crossing boundary regions is:

1. Choose a set of non-crossing regions of the boundary to calculate the entropies of. Recall that this means that for any two chosen regions, either they are disjoint, or one is nested inside

of the other. In the bulk, determine the minimal surfaces homologous to each boundary region and denote them $m(B)$. It is important to note that since the boundary regions are non-crossing, the regions given by the interior of $B \setminus m(B)$ also do not cross for any two choices of B .

2. Now note that the boundary regions and minimal surfaces divide the entirety of the bulk into a finite number of "cells." In the case where the boundary regions are non-crossing, there are a few different cases for these cells.

- (a) The cell is the interior of $B \setminus m(B)$ for some choice of B .
- (b) The cell is bounded by the minimal surface of some boundary region which has other source regions nested within it. In this case, the form of the cell is not that of (a), but instead, the cell is now given by

$$\text{Int } B \setminus m(B) \cap \bigcap_{B' \subset B} \text{Int } B' \setminus m(B') : \quad (43)$$

In general, these cells will be bounded by the minimal surface of $m(B)$, some subset of B itself, and the minimal surfaces of the regions nested within B .

- (c) The last type of bulk cell which we will encounter for non-crossing regions is bounded by none of the source boundary regions, but rather bounded by the interior of the union of the purifying region and its minimal surface. In other words, this last cell type is the complement of the union of all other bulk cells.
3. Constructing a maximal thread configuration for each individual bulk cell is straight forward if we make use of Theorem 1 from [4]. This theorem tells us that for any number of disjoint regions, there exists a multi flow (or thread configuration) that is simultaneously maximized on all of them. Since the proof of this theorem is completely independent of the bulk/boundary geometry, we are free to apply it to individual bulk cells. Based on the cells described in step 2, we can choose our 'sub-source regions' for each bulk cell to be either a minimal surface of some source region or some subset of our source region. This gives us a decomposition of the boundary of each bulk cell into disjoint regions.

Now for each region bounding each bulk cell we make use of the theorem from [4] to construct/state the existence of a thread configuration which is maximal for all boundaries of each cell.

4. Now that we have a maximal thread configuration for each bulk cell, we must now recombine them and show that this thread configuration is maximal for each source region. We do this by taking note of the following facts:

- (a) Since any minimal surface is the minimizer of its homology class, we know that the maximum number of threads which can be placed on them is equal to their area. This means that any thread configuration which maximizes on a minimal surface will have the threads maximally packed everywhere on it.
- (b) By virtue of how we have divided the bulk, every minimal surface forms part of the boundary of exactly two bulk cells.

- (c) Because of (a) and (b) when two adjacent bulk cells are recombined, the density (and direction) of threads on their shared boundary will be equal and maximal. This allows us to put the bulk cells back together and think of the thread configurations on the individual bulk cells as being continuous over their shared boundaries.
5. Thus stitching together to maximal thread configurations on each individual bulk cell gives us a well defined thread configuration for the entire bulk. The fact that there is no crossing in our chosen source regions ensures that their minimal surfaces will not cross either. Thus once a thread leaves a one bulk cell it will not return to it from another one when the bulk is stitched back together. This means that no threads will loop back to the boundary region they leave from. If this were not the case the proof would fail since threads which return to the boundary they leave from correspond to closed lines with net zero flux. The fact that no thread returns to a region it leaves is clear from the fact that the graph model describing this setup is a tree graph if no crossing is present. Since this is the case and thread configuration is maximized on all of the minimal surfaces of the source regions (by construction), and the entire thread configuration must be maximal for all source regions.
 6. Now all that is left to do is to convert this thread configuration into a proper multi flow by choosing an orientation for the threads. Once this is done, the construction is complete and the proof is concluded.

4 Multiflows for Crossing Regions

Since multi flows are capable of computing the entropy of arbitrary non-crossing regions, we can now ask if they can do the same for crossing regions. In order to test this, we will consider a relatively simple problem.

The machinery of convex optimization and multi flows make no reference to any particular geometry, and so we are free to work in a simpler geometry than AdS. With that in mind, we consider the unit square on \mathbb{R}^2 given by $(0;1)^2$. We label the sides of this square $A; B; C$ and D , and define a multi flow on this square; $f_{ij}g$ where $i; j \in \{A; B; C; D\}$. Note that the entropy of any single region on its own is given by;

$$S(A) = S(B) = S(C) = S(D) = 1 \tag{44}$$

since the minimal surface of each is simply the region itself. Furthermore, the entropy of the union two adjacent sides are equal to

$$S(AB) = S(AD) = S(BC) = S(CD) = \frac{\rho_-}{2}; \tag{45}$$

as displayed in Figure 7. In order to test multi flows in the case of crossing source regions in this toy problem, we attempt to maximize the flux of a multi flow on this square over the crossing source regions AB and BC . If multi flows are capable of simultaneously computing the entropy of two crossing regions, we should expect that the maximal flux from these source regions should be $S(AB) + S(BC) = 2 \cdot \frac{\rho_-}{2}$. Approaching this problem can be done in two ways; attacking it head on, or dualizing the problem and trying to find a solution to that. We will do both, starting with analytic ansatzes and then attempting to numerically compute the solutions for both the primal and the dual on a lattice.

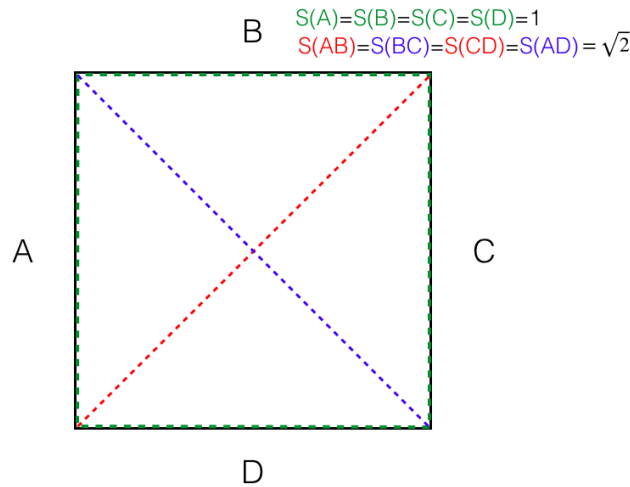


Figure 7: An illustration of the minimal surfaces and corresponding entropies of the toy problem described.

4.1 Analytic Attempt: Primal

Before beginning, note that the convex program in question is this:

$$\text{Primal: Maximize } \int_{AB} v_{(AB)(CD)} + \int_{BC} v_{(BC)(AD)} \text{ with respect to } \{v_{ij}\} \text{ subject to}$$

$$v_{ij} \geq 0; \sum_{i < j} v_{ij} = 1.$$

We may rewrite the objective of this program as

$$\int_{AB} (v_{AC} + v_{AD} + v_{BC} + v_{BD}) + \int_{BC} (v_{BA} + v_{BD} + v_{CD} + v_{CA}) \quad (46)$$

$$= \int_A (v_{AB} + 2v_{AC} + v_{AD}) + \int_B (v_{BC} + 2v_{BD}) + \int_C v_{CD}:$$

There are two important things to consider for formulating an ansatz for this problem. First, note that the square itself exhibits the full range of symmetries of the Dihedral-4 group, thus there should exist a maximal solution which exhibits the same symmetries. We may restrict ourselves to ansatzes which do so, thereby narrowing the range of possible solutions. Secondly, note that the flows v_{AC} and v_{BD} contribute twice as much as the other flows in the objective function.

This second fact is misleading in some ways, as one may assume that the maximal solution will be one with both of these flows dominating the bulk. However, note that only one of them can be saturated on the entire square at once. There are three things one may try to get around this;

1. Make all flows zero except for one of these two (say v_{AC}) which has magnitude one on the entire square. This gives a total flux of $2 < 2\sqrt{2}$.
2. Compromise and make both flows v_{AC} and v_{BD} non-zero with magnitude $\frac{1}{2}$ everywhere. This too gives a total flux of $2 < 2\sqrt{2}$.

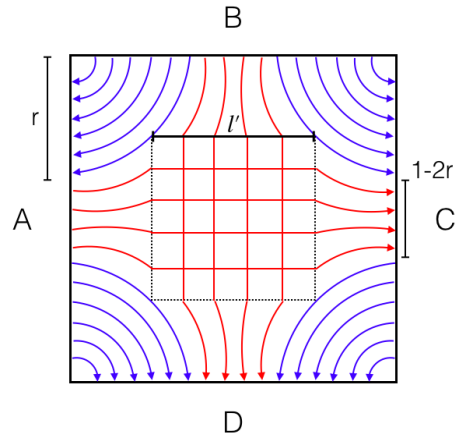


Figure 8: An illustration of our maximal ansatz. Flows between opposite sides of the square are shown in red and flows between adjacent sides in blue. Note that the density of the flow lines going across the square is maximal at the boundary but less in the interior of the square. In order to give l' the necessary value of $l' = 2(1 - 2r)$ we choose $r = \frac{1}{4-\sqrt{2}}$. This gives a total flux of $4\left(\frac{3-\sqrt{2}}{4-\sqrt{2}}\right)$.

Evidently, these double-counted flows alone will not give a maximal solution (unless the maximum flux is 2). Next we might guess that the flows between adjacent sides, which are only counted once in the objective, form quarter circles of radius r about the corners of the square. A quick check confirms that if these are the only flows in the system the maximal value of the flux is once again 2.

For a more sophisticated guess, we maintain that the flows between adjacent sides will flow in quarter circles in which the norm bound is saturated, but now we have nonzero flows from opposite sides as well. The symmetry suggests that these cross flows must be equal at the center of the square and thus their magnitude there cannot exceed $\frac{1}{2}$. In order to maximize the flow between opposite sides, we can imagine giving the flows a norm of 1 on the available space on the boundary and then having the threads spread out as space is made available for them. This will continue up to the point where they are no longer restricted by the flows between adjacent sides. From there, we assume for simplicity that the threads will flow uniformly across the square until obstructed again. In order to accomplish this, we can imagine placing a smaller square concentrically inside the unit square such that within it the flows between opposite sides are uniform and of magnitude $\frac{1}{2}$. The size of this square is limited by the radius of the quarter circles formed by the flows between adjacent sides. Such a configuration is depicted in Figure 8.

A very brief geometrical calculation tells us that, in order for the flows between opposite sides to have magnitude 1 on the boundary and $\frac{1}{2}$ in the center, we must choose a radius $r = \frac{1}{4-\sqrt{2}}$ for the quarter circles formed by the flows between adjacent sides. This is such that $l' = 2(1 - 2r)$ where l' is the side length of square enclosing the uniform cross-flow.

This configuration gives a total flux of

$$Z_{AB} V_{(AB)(CD)} + Z_{BC} V_{(BC)(AD)} = 4 \left(\frac{1}{4} \rho_{\bar{2}} \right) + 4 \left(\frac{1}{4} \rho_{\bar{2}} \right) = 2.453 \quad (47)$$

Which is larger than 2 but still less than the expected value of $2\sqrt{2}$.

We can imagine improving this ansatz by making the ways the flows behave a little less rigid and discontinuous, but to do this analytically is not feasible. Instead, we can dualize this problem in order to see if we can really achieve our desired goal of calculating the entropies of the two crossing regions simultaneously.

4.2 Analytic Attempt: Dual

We dualize our program in the usual way of removing the constraints and adding them into the objective multiplied by Lagrange multipliers and then maximizing with respect to the usual variables.

$$L = \sum_{i=1}^M \sum_{j>i} v_{ij} + \sum_{i=1}^M \sum_{j>i} r_{ij} (v_{ij} - 1) + \sum_{i=1}^M \sum_{j>i} j v_{ij} \quad (48)$$

Where $A_1 = A$; $A_2 = B$, etc. By performing integration by parts on the second term in the Lagrangian and demanding that the resulting boundary terms vanish (to ensure that our maximum flux is finite) we gain the conditions:

$$A_1 B_1 A_2 = A_1 C_1 A_2 = A_1 D_1 A_2 = B_1 C_1 B_2 = B_1 D_1 B_2 = C_1 D_1 C_2 = 1 \quad (49)$$

$$A_1 B_1 B_2 = A_1 D_1 D_2 = B_1 C_1 C_2 = C_1 D_1 D_2 = 0$$

$$A_1 C_1 C_2 = B_1 D_1 D_2 = 1$$

And we are left with a Lagrangian

$$L = \sum_{i=1}^M \sum_{i<j} (v_{ij} - r_{ij} + j v_{ij}) \quad (50)$$

This is maximized with respect to the flows when v_{ij} is anti-parallel to r_{ij} , at which point if we want the maximum of our program to be finite we better require that

$$j r_{ij} \leq 0 \quad \forall i, j \quad (51)$$

At this point the maximum value of the Lagrangian occurs when all flows are equal to zero and we are left with the objective of our dual program;

$$Z = \sum_{i=1}^M \sum_{i<j} j \quad (52)$$

which we will minimize with respect to r_{ij} and j subject to the constraints given by equations (51) and (49).

Note that these constraints together imply that for the path integral of $\int_c ds$ along some path c ;

$$\int_c ds \quad \begin{cases} 1 & c \text{ connects adjacent sides of square} \\ 2 & c \text{ connects opposite sides of square:} \end{cases} \quad (53)$$

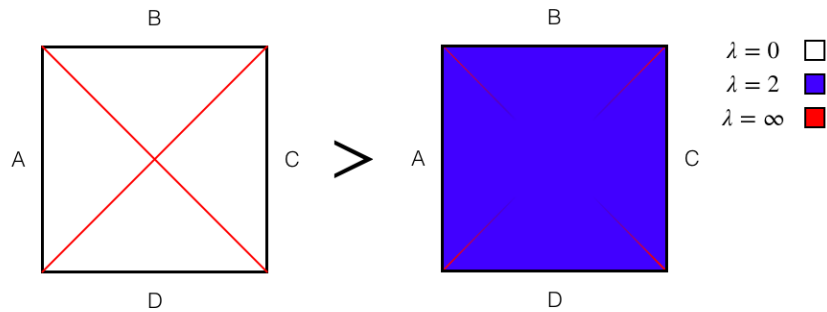


Figure 9: Illustration of ansatzes for the dual program. On the left is the configuration we expect based on the Locking Theorem. Here λ is zero everywhere except for on the minimal surfaces for AB and BC , where it is infinite. On the right is an example of a feasible λ which returns a smaller value of the objective. Most everywhere $\lambda = 2$ except for delta functions coming from the corners which have a weight which decreases linearly with distance from the corner.

This lets us rephrase the dual program in as

$$\text{Minimize } \int_M \lambda \text{ with respect to } \lambda \text{ subject to equation (53).}$$

Recall that if the primal program is to return the sum of the entropies of the regions sourcing the multi flow, then the dual program should return the same. The λ that minimizes the dual program should be a delta function located on those surfaces and zero everywhere else in the bulk. For this problem then, we hope that λ consists of delta functions connecting opposite corners of the square, which would give $2\sqrt{2}$ when integrated over the entire square. If there is a choice of λ which satisfies the constraints given and has an area integral less than $2\sqrt{2}$ then the objective of our primal program will be bounded above by this value. Thus the multi flows will fail to compute the entropies of the crossing regions.

If we try to think of such a λ we may be tempted to start by making λ take a constant value of 2 everywhere. This would automatically satisfy the constraint for paths connecting opposite sides of the square, however it does not satisfy the constraint on all paths between adjacent sides. Simply stated this is because the minimum length of a path connecting opposite sides is 1 while the minimum length of paths connecting adjacent sides is infinitesimal. Thus we know that any feasible λ must go to infinity at the corners of the square.

As an extension of this thought, we can place delta functions along the lines connecting opposite corners of the square which are weighted such that they ensure that paths between adjacent sides are ensured to be greater than 1 when integrated against λ . In doing this calculation we find that the appropriate weight to add to these delta functions is

$$\frac{1}{2\sqrt{2}}; \tag{54}$$

where r is the distance from the nearest corner of the square. Note that at $r = \frac{1}{2\sqrt{2}}$ the delta function ends. Integrating this weight from 0 to $\frac{1}{2\sqrt{2}}$ tells us that each one of these four

weighted delta functions contributes $\frac{\rho_{\bar{2}}}{8}$ to the objective. Thus for this ansatz we have

$$\begin{aligned} Z_M &= 2 + 4 \frac{\rho_{\bar{2}}}{8} = 2 + \frac{\rho_{\bar{2}}}{2} \quad 2.707 < 2^{\rho_{\bar{2}}/2} \end{aligned} \quad (55)$$

Since the value of the objective function of the dual program for any feasible point gives us a strict upper bound of the maximum of the primal objective function, this lets us conclude that the multi flow formalism fails to compute the entropies when presented with crossing regions (or at the very least will not always be successful). We can ask what the actual solution to the problem is if not the entropies of the source regions. Since our analytic ansatzes are likely not the true solutions, our best bet is to turn to numerical optimization to find an answer.

4.3 Numerical Check: Dual

4.3.1 Implementation

For all numerical work we have used the optimization tools built into *Wolfram Mathematica* (11). To numerically compute the optimum of the dual and primal programs, we first discretize the unit square to an $L \times L$ lattice. What variables we define on these lattice sites will change between the computation of the primal and dual programs. For both programs we will find the solution to the optimization problem for increasing values of L (doing so effectively increases the 'resolution' of our computation).

We will start with our treatment of the dual program. In performing this exercise, we hope to learn how far the optimum of our primal program is from the expected value of $2^{\rho_{\bar{2}}/2}$ as well as get a sense of the form of ϕ which gives the minimum of the dual program to see what we can learn from it. For the computation, we will implement the dual program in the form of equation (52) subject to the constraints (49) and (51). On each lattice site we define the variables $\chi_{XY}(i;j)$, where $X; Y \in \{A; B; C; D\}$ and $i; j \in \{1; 2; \dots; L\}$, and impose the appropriate boundary conditions on each χ_{XY} on the outermost lattice sites. When X and Y represent adjacent sides of the square, we assign to χ_{XY} a value of half the difference between its two boundary values at the corner where X and Y meet. Now we can compute the magnitude of the gradient of each χ_{XY} on the plaquette (the set of which we can think of as an $(L-1) \times (L-1)$ lattice). The numerical magnitude of gradient of χ_{XY} on the plaquette labeled by $(i;j)$ is given by

$$\chi_{XY}(i;j) = \frac{L-1}{2} \left(\chi_{XY}(i+1;j+1) - \chi_{XY}(i;j) \right)^2 + \left(\chi_{XY}(i;j+1) - \chi_{XY}(i+1;j) \right)^2 \frac{1}{2} \quad (56)$$

We also define variables $\phi(i;j)$ on each plaquette and constrain them by the magnitude of the gradient of all χ_{XY} on the $(i;j)$ th plaquette.

The last thing we must do before proceeding with the computation is define our objective. The integral of ϕ over the square is given by

$$\text{Objective} = \frac{1}{(L-1)^2} \sum_{i,j=1}^{L-1} \phi(i;j) \quad (57)$$

Doing this has fully defined the dual program numerically, so all that is left to do is feed the information into Mathematica's built in optimization tools. Before this is done, however, it is

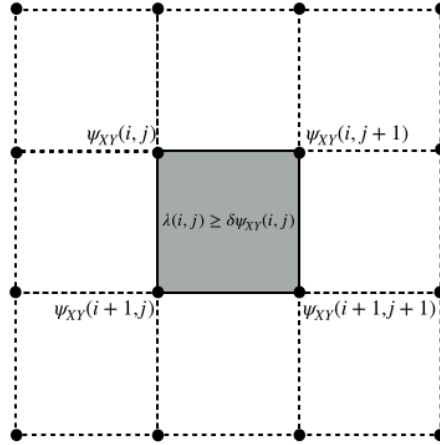


Figure 10: Each site on the $L \times L$ lattice has the variables ψ_{XY} . These are used to constrain the λ in the square enclosed by neighboring lattice points.

worth noting that we have defined $6(L^2 - 2L) + (L - 1)^2$ variables to minimize with respect to. Obviously this will grow rapidly as we increase L , so it is in our best interest to reduce the number of variables in our program for the sake of efficiency of computation. Luckily, we have yet to consider the many symmetries of our problem. Doing so will allow us to reduce the number of variables tremendously.

If we want to compute a solution which obeys all the symmetries of our system, we can first say that out of the six ψ_{XY} we have defined, only two of them are really independent. This lets us consider only ψ_{AB} and ψ_{AC} . The other four ψ_{XY} are related to these two by rotations and reflections. Additionally, we can say that since the λ which will result from our computation should be symmetric under elements of the Dihedral-4 group, we only need to compute it on one eighth of the square, as shown in Figure (11).

Once these changes were implemented, we computed the solution to the program for a number of lattice sizes. As expected from our analytic endeavors, we found that the λ which gave the minimum objective value was not the given by a delta function along the minimal surfaces of AB and AC , but rather a much more complicated function.

4.3.2 Results

Qualitatively, it appears that the true minimal solution retains some of the cross structure from the minimal surfaces we were expecting to find, but much more relaxed and spread out. We found that the λ did indeed begin to diverge towards infinity in our numerical solution, as it must. In addition there is a local maxima at the center of the square and a raised ridge connecting this maxima to the corners, giving the function a slight cross-like feature. There is also a set of local minima which are displaced from the center of each side of the square.

We can analyze the structure of this solution by considering the condition of complementary

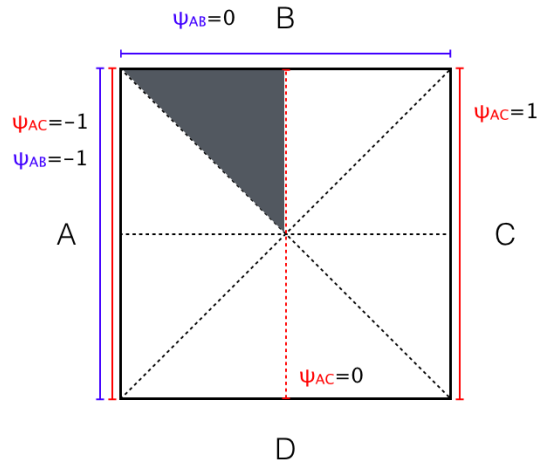


Figure 11: The symmetries of the square allow us to do our computation only for the shaded triangle in the figure. The solution on the rest of the square will be related to that on this triangle by rotations and reflections. The boundary conditions for the independent ψ_{XY} s are also shown. We gain a new boundary condition on ψ_{AC} from symmetry.

slackness [5], which tells us that

$$(1 - \sum_{X=1}^4 \sum_{Y>X}^4 j_{XY} \psi_{XY}) = 0 \quad (58)$$

at every point on the square. In this way, ψ acts a measurement of how much (or how little) the norm bound on the multi flows is saturated in the corresponding optimum of the primal. If $\psi = 0$ anywhere, this must then mean that at this point the sum of the magnitudes of all the flows in the primal solution will be less than 1. If ψ is greater than zero, then they must sum to exactly one. The higher ψ is at a particular point, the more 'pressure' the norm bound is putting on the multi flows at that particular point.

Using this to guide our analysis of the solution to the dual is useful in a few respects, but one is particularly noteworthy. In the solution we compute, ψ is nowhere zero. Thus the multi flow that maximizes the primal program must saturate the norm-bound everywhere on the square, which was not true in our analytic ansatz.

The maximum lattice size we computed a solution for $L = 33$ and this gave an objective value of 2.532. A contour map of the ψ found from this is shown in Figure 12.

4.4 Numerical Check: Primal

4.4.1 Implementation

Now that we have a numerical solution to the dual program, there are a few good reasons to compute that of the primal. Firstly, we can check that the numerical solution to the primal

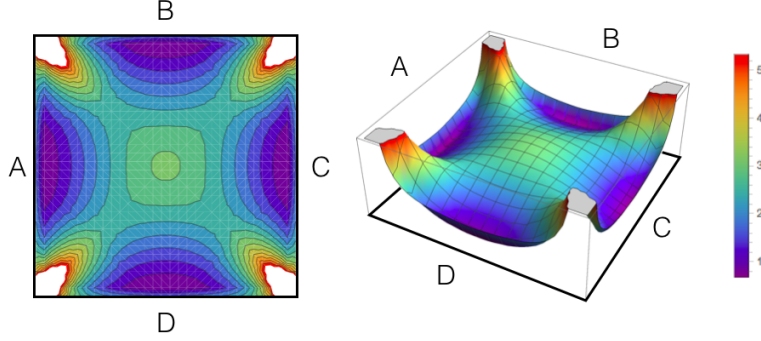


Figure 12: Left: A contour map giving the minimal value of the objective on a $L = 33$ lattice. Right: A 3D plot of the same.

program has a solution which is consistent to that of the dual. Secondly, looking at the maximal multi flow configuration for the program may give us some insight into why the multi flow formalism is unable to compute the entropies for crossing source regions.

We may once again make use of the symmetries of the square to pare down the number of variables that are optimized over. Instead of computing all six flows, we can get away with computing only two: one between adjacent sides and one between opposite sides of the square. All other flows will be related to these by reflections and rotations. We choose to compute v_{AB} and v_{AC} explicitly.

To actually compute these flows and the flux through the corresponding regions, it is easiest to define pseudoscalar streamfunctions for the flows, the curl of which are the flows themselves.

$$\Gamma_{XY} = \nabla_{XY} \psi_{XY} \quad (59)$$

Note that this is only permissible because we are dealing with divergenceless vector fields in two dimensions.

There are a few important properties of the streamfunction which will come in handy. First, as alluded to above, this definition of the flows in terms of streamfunctions automatically guarantees that the flows will be divergenceless. Second, the magnitude of the the curl of the streamfunction is equal to that of its gradient. Thus

$$|\nabla_{XY} \psi_{XY}| = |\Gamma_{XY}| = |\nabla_{XY} \psi_{XY}| \quad (60)$$

So we can compute the magnitude of gradient on the lattice for use in imposing the norm-bound on the multi flow, similar to how we imposed the lower bound on ψ in the dual program. Lastly, the fact that flow v_{XY} will have no flux through a boundary Z if $Z \notin X; Y$ tells us that the corresponding streamfunction will be constant along that boundary. By enforcing this, we can define a variable ψ_{XY}^0 which represents the constant value taken by the streamfunction on some boundary. By demanding that the streamfunction be zero on another boundary, or at some appropriate point, we can use the fundamental theorem of calculus to write

$$\int_x^Z \nabla_{XY} \psi_{XY} = \int_x^Z \Gamma_{XY} = \psi_{XY}^0 \quad (61)$$

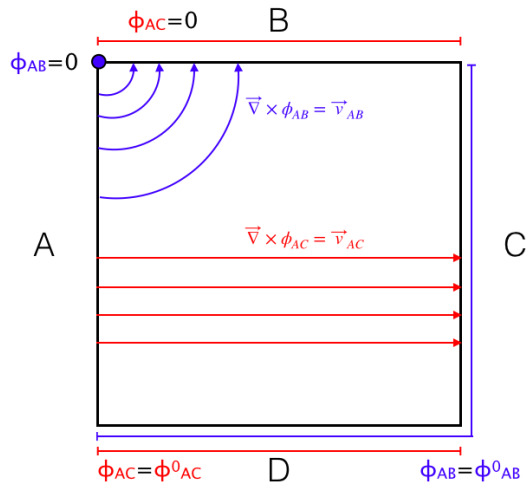


Figure 13: We define streamfunctions on the square, which will ensure that the resulting flows are divergenceless. The boundary conditions on the streamfunctions ensure that the flows have flux through the appropriate regions. Allowing the streamfunction to take a constant, but undetermined value at one boundary will allow us to compute the total flux of the resulting flow field.

This lets us express the objective of the primal program as

$$\sum_{AB} V_{(AB)(CD)} + \sum_{BC} V_{(BC)(AD)} = 4(\phi_{AB}^0 + \phi_{AC}^0): \quad (62)$$

The factor of 4 is included to account for the fact that we only compute two of the six flows, as well as the fact that the flows between opposite sides are weighted twice as heavily as the others.

All that is left to do now before performing the computation is to impose the constraint on the norm of the flows. This turns out to be a non-trivial task. One complication arises from a quirk of Wolfram Mathematica's built in optimization functions. The norm-bound constraint is a sum of absolute values, which is not a smooth function. If this is not corrected, Mathematica's optimization functions would return strange, often non-feasible, solutions or worse yet, would fail entirely. In order to correct for this, we can 'smooth' out the norm-bound constraint by changing it to

$$\sum_{x=1}^X \sum_{y>x}^Y \rho \frac{1}{\sqrt{\epsilon v_{xy}^2 + 1}} \quad (63)$$

We fix the value of epsilon to be sufficiently small that it does not change the solution very much, but sufficiently large as to resolve the problem described. For the work described here we set $\epsilon = 0.001$.

A second complication with imposing the norm-bound on the lattice comes about when we consider the consequences of how we have calculate the magnitude of gradients on the lattice. If we choose to compute the gradients of v_{xy} in a fashion similar to the one used for the dual

program (56), then one will realize that adding any constant to a function at lattice sites $(i;j)$ and $(i+1;j+1)$ will not change the value of the gradient. However, this constant can change the value of the objective. Mathematica's optimization procedure will make use of this, giving rise to strange solutions with objective values above that of the true solution.

To avoid this, we calculate the magnitude of the gradient of χ_Y in a number of different ways and impose norm-bounds on all of them. The magnitudes we calculated are:

$$\begin{aligned}
 1 \quad \chi_Y(i;j) &= (L-1)^p \frac{(\chi_Y(i+1;j) - \chi_Y(i;j))^2 + (\chi_Y(i;j+1) - \chi_Y(i;j))^2}{(L-1)^p}; \\
 2 \quad \chi_Y(i;j) &= (L-1)^p \frac{(\chi_Y(i+1;j+1) - \chi_Y(i+1;j))^2 + (\chi_Y(i;j+1) - \chi_Y(i+1;j))^2}{(L-1)^p}; \\
 3 \quad \chi_Y(i;j) &= (L-1)^p \frac{(\chi_Y(i+1;j+1) - \chi_Y(i;j+1))^2 + (\chi_Y(i;j) - \chi_Y(i;j+1))^2}{(L-1)^p}; \\
 4 \quad \chi_Y(i;j) &= (L-1)^p \frac{(\chi_Y(i+1;j+1) - \chi_Y(i;j+1))^2 + (\chi_Y(i+1;j) - \chi_Y(i+1;j+1))^2}{(L-1)^p};
 \end{aligned} \tag{64}$$

This step completes the implementation of the primal program in Mathematica. We now proceed to compute the solution to the program on lattices of increasing size.

4.4.2 Results

Starting at $L = 5$ we doubled the resolution until finally performing the optimization on an $L = 65$ lattice. This resulted in an objective value of ≈ 2.502 , which is consistent with the result from the computation of the dual program. A quick check of the maximal flow configuration confirms that the norm-bound is saturated everywhere on the square, as suggested by our analysis of the solution of to the dual program. By plotting the contours of χ_Y we can see the streamlines of \forall_{XY} , which corresponds to the arrangement of the bit threads.

The thread configuration we find appears to be similar to our analytic ansatz for the primal. The flows between adjacent sides are the square form quarter circles centered at the corners. In addition to this, the flows between adjacent sides start concentrated at the boundary of the square where space is available and spreads out to half the density in the center of the square. The maximal thread configuration for a $L = 65$ lattice is shown in Figure (14).

5 Discussion and Future Work

For both the primal and dual programs we computed solutions numerically on lattices of different sizes. Plotting the value of the optimum primal and dual objectives for different lattice sizes shows how the optima converge on the lattice. This is shown in figure 15. Based on this, we are confident that both the result for the primal and dual programs reflect the qualitative form of the optimal solution as well as a descent estimate of the optimum value of the objective functions.

Based on this work, the Locking Theorem represents the point at which multi flows in the continuum begin to yield results which differ from their discrete counterparts. In fact, outside of actually finding the solution given to us by multi flows for a simple problem, there were other clues which signaled that crossing regions may present a problem.

The most notable of these is built into the method used to prove the Continuum Max-Flow Min-Cut theorem for some choice of source regions, an example of which is given by the dualization proof in Section 3. These proofs rely on the fact that we can identify the level sets of $\chi_{ij}(x)$

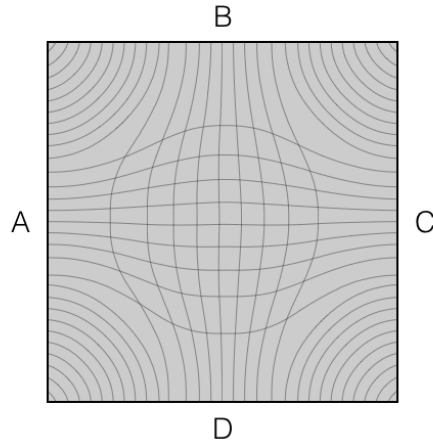


Figure 14: The maximal thread con guration of the primal program as given by the contours of the streamfunctions χ_Y .

which are homologous to each source region, and that the regions composed of them do not cross. However if we have crossing regions, then any curves homologous to the two crossing regions must intersect one another. While this was not a death sentence for the idea that multi ows may be able to calculate the entropies for crossing regions, it certainly signals that the issue is non-trivial.

With the question of whether or not multi ows satisfy a 'Continuum Locking Theorem' answered, we are left to wonder why it is that we have reached this conclusion. For answers, we turn back to thinking about a graph model for holographic entanglement entropies.

Knowing the relevant minimal surfaces for the square problem (see Figure 8) allows us to construct a graph model for the square in the way described in Section 2. On this graph we have terminals which represent the regions A ; B ; C and D and we can ask the discrete version of our original question. What is the maximal commodity ow we can send from AB to CD and from BC to AD simultaneously. Of course, the Locking Theorem along with Max-Flow Min-Cut assures us that this will end up being $2\sqrt{2}$. An example of a con guration in which this is achieved is shown in gure 16. With this we can ask; why isn't an analogous con guration possible in the continuum?

While commodity ows on graphics are either parallel or anti-parallel to each other, a ow in the continuum can take on other orientations relative to another ow. This leads to problems wherever two RT surfaces cross in the bulk. Recall that in order for a ow to successfully calculate the entropy of a source region it must have a norm a 1 and be perpendicular to the minimal surface everywhere on the surface. Of course, these two features can not be accomplished simultaneously on two minimal surfaces which cross one another.

In order to further the ability of the continuum multi ow, we may consider changing its de nition in some respects in an attempt to address this breakdown between the continuum and the discrete. This would be accomplished by modifying the constraints which de ne the multi ow, the most notable being the collective norm-bound

$$\sum_i |v_i| \leq 1 \tag{65}$$

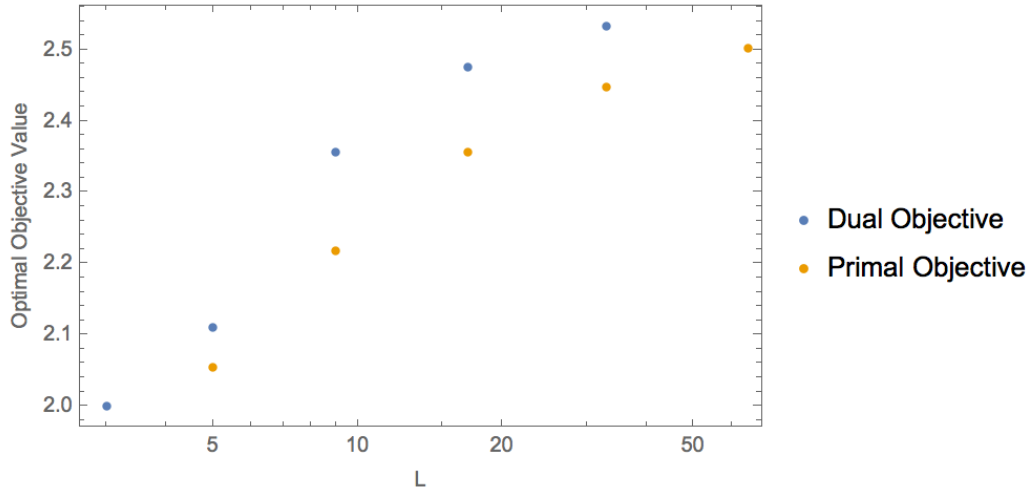


Figure 15: Plot showing optimal value of programs as a function of lattice size L .

This norm-bound is by far the simplest one to work with for multi-ows, but it may not be the most physically significant. As part of future work, we will be considering norm bounds of the form

$$\prod_i |v_i \cdot \hat{n}_i| \leq 1 \quad (66)$$

where \hat{n} is a unit vector. Physically, this constraint is the statement that the number of bit threads passing through a surface must not exceed the area of the surface divided by the area of one thread. This is perhaps a more natural constraint for multi-ows. It is a weaker constraint than the current norm-bound, but maintains the property that each component of a multi-ow is itself a-ow. In fact, with this norm bound, we can create a continuum multi-ow which is analogous to the discrete commodity-ow configuration pictured in Figure 16 in which there is a uniform-ow between A and C and another between B and D , both with norm $\frac{\rho}{2}$. This could be a hint that this norm-bound is the more physically relevant one and should be adopted in place of the current constraint.

We must also acknowledge the possibility that, in order to perform entropy computations for more complicated arrangements of source regions, we may need a new structure altogether. One possibility is that this may be achieved by imposing a weaker constraint on the divergence of multi-ows. It could be the case that we require something like a multi-ow, but which has non-zero divergence governed by some rules or perhaps even another field. In order to cover all bases, this must also be considered as a possibility even if its physical meaning, or even its form is not immediately apparent. Regardless, we will explore both possibilities going forward in an attempt to strengthen the multi-ow formalism and our understanding of the information structure of holographic states.

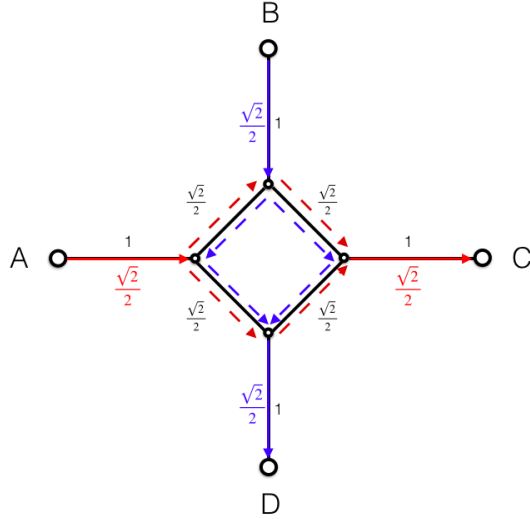


Figure 16: An example of a multi-commodity flow configuration which is maximal for both source regions AB and BC on the graph model corresponding to the square. The edge capacities are shown in black and the commodity flows in blue and red.

6 Acknowledgements

We'd like to thank Professor John Wilmes for his advice on numerical methods in convex programming as well as Jonathan Harper for very helpful discussions on numerous facets of this project as well as comments on earlier drafts of this work.

7 References

- [1] Ning Bao, Sepehr Nezami, Hiroshi Ooguri, Bogdan Stoica, James Sully, and Michael Walter. The holographic entropy cone. *Journal of High Energy Physics*, 2015(9):130, Sep 2015. arXiv:1505.07839v1.
- [2] Michael Freedman and Matthew Headrick. Bit threads and holographic entanglement. *Communications in Mathematical Physics*, 352(1):407{438, May 2017.
- [3] G. Naves. "notes on the multicommodity flow problem". http://assert-false.net/callcc/Guyslain/Works/multi_flows.
- [4] Shawn Cui, Patrick Hayden, Temple He, Matthew Headrick, Bogdan Stoica, and Michael Walter. Bit threads and holographic monogamy. arXiv:1710.09516, 8 2018.
- [5] Matthew Headrick and Veronika E Hubeny. Riemannian and lorentzian flow-cut theorems. *Classical and Quantum Gravity*, 35(10), Apr 2018.